Title

OPTICAL-FIELD-INDUCED REFRACTIVE INDICES and ORIENTATIONAL RELAXATION TIMES IN A HOMOLOGOUS SERIES OF ISOTROPIC NEMATIC SUBSTANCES

Author

Hanson, E.G.

Publication Date

1976-02-01

Submitted to Physical Review

LBL-4914
Preprint

OPTICAL-FIELD-INDUCED REFRACTIVE INDICES AND ORIENTATIONAL RELAXATION TIMES IN A HOMOLOGOUS SERIES OF ISOTROPIC NEMATIC SUBSTANCES

E. G. Hanson, Y. R. Shen, and G. K. L. Wong

February 1976

Prepared for the U. S. Energy Research and
Development Administration under Contract W-7405-ENG-48

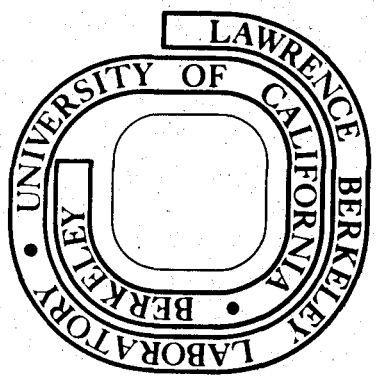

DISCLAIMER

OPTICAL-FIELD-INDUCED REFRACTIVE INDICES AND ORIENTATIONAL RELAXATION TIMES IN A HOMOLOGOUS SERIES OF ISOTROPIC NEMATIC SUBSTANCES.*

E. G. Hanson and Y. R. Shen†
Department of Physics, University of California, and
Materials and Molecular Research Division,
Lawrence Berkeley Laboratory, Berkeley, California 94720

and

G. K. L. Wong
Physics Department
Northwestern University
Evanston, Ill.

ABSTRACT

We have measured the optical Kerr constant and the orientational relaxation times of seven p,p'-di-n-alkoxy-azoxybenzene homologous compounds as functions of temperature in the isotropic phase. The observed critical behaviors near the isotropic-nematic transitions agree well with the predictions from the Landau-de Gennes model. Various characteristic parameters of the homologues are deduced from the experiment. Their variations with increase of methylene groups in the alkyl chain are discussed. Our results suggest that neither the mean-field theory of Maier-Saupe nor the Landau expansion of free energy is a good approximation for quantitative description at the isotropic-nematic transition.

*Supported by The National Science Foundation Grant No. DMR74-07361.

†On leave at The Miller Institute of University of California.

I. INTRODUCTION

Recently, it has been demonstrated by nonlinear optical measurements that liquid crystalline materials in their isotropic phase can have a large optical Kerr constant with a long relaxation time.[1] Such characteristics result from the pretransitional behavior of the materials. The nonlinear optical measurements actually provide a stringent test on the Landau-de Gennes phase transition model for liquid cyrstals. From these measurements together with measurements on the order parameter and anisotropy in refractive indices, one can obtain values for large number of characteristic material parameters: T^*, the fictitous second-order isotropic-nematic transition temperature; ν, the viscosity coefficient for molecular orientation; a, b, and d, the coefficients in the Landau's series expansion of the free energy; and others. These parameters are important for characterizing a liquid crystalline material. To understand how molecular structure affects the properties of liquid crystals, it will then be of great interest to find these parameters for a homologous series of compounds. However, no such information for any homologous series exists in the literature.

In this paper, we report the results of our recent nonlinear refractive index measurements on the homologous compounds of p,p'-di-n-alkoxy-azoxybenzenes. The molecular structures of these compounds are shown in Table I. Also listed in the Table are the isotropic-nematic transition temperatures T_K of our samples, the macroscopic order parameters Q_K at T_K, the refractive index anisotropies Δn (defined for

the case of perfect molecular alighment) we recently measured, and the latent heats ΔH obtained from Ref. 2. From the nonlinear optical measurements and the values of T_K, Q_K, and Δn , we then deduce the various characteristic parameters we mentioned earlier for these homologous compounds. The work here constitutes one of the very few examples where nonlinear optical measurements can yield quantitative results not only on nonlinear optical coefficients but also on other characteristic parameters of a condensed matter.

In Sec. II, we give a brief review on the theory of optical field-induced refractive indices. We describe in Sec. III, the experimental arrangement and the data analysis procedure. Then, in Sec. IV, we present the experimental results and the material parameters deduced from our results. Finally, Sec. V discusses the implications of our results from the molecular structural view point.

II. THEORETICAL BACKGROUND

Liquid crystalline materials are composed of highly anisotropic molecules. Consequently, the induced dipoles on the molecules are also highly anisotropic. In the presence of intense optical field, the molecules tend to be aligned by the field via induced dipole interaction with the field. The resultant molecular ordering is then reflected by the induced optical anisotropy in the medium.

If Q is a macroscopic tensorial order parameter which describes the degree of molecular alignment, then the optical susceptibility

χ_{ij} (or any tensorial property of the medium) can be written as[3]

$$\chi_{ij} = \bar{\chi}\delta_{ij} + \frac{2}{3}\Delta\chi Q_{ij} \qquad (1)$$

where $\bar{\chi} = \frac{1}{3}\Sigma_i \chi_i$ and $\Delta\chi$ is the anisotropy in χ_{ij} with perfect molecular alignment such that $\frac{1}{2}Q_{xx} = -Q_{yy} = -Q_{zz} = 1$. In the absence of field, in an isotropic medium, Q_{ij} is zero, but becomes finite in the presence of a field. According to the Landau-deGennes model,[2] the free energy per unit volume of an isotropic fliud in the presence of an intense field $\vec{E}(\omega)$ and a weak probing field $\vec{E}(\omega)$ is given by

$$F = F_o + a(T - T^*)Q_{ij}Q_{ij} + \frac{1}{3}bQ_{ij}Q_{jk}Q_{ki} + \frac{1}{4}dQ_{ij}Q_{jk}Q_{kl}Q_{li}$$

$$- \frac{1}{4}\chi_{ij}(\omega)E_i^*(\omega)E_j(\omega) - \frac{1}{4}\chi_{ij}(\omega')E_i^*(\omega')E_j(\omega') \qquad (2)$$

where F_o is independent of Q. The field-induced molecular ordering then obeys the dynamic equation[3] $\nu\partial Q_{ij}/\partial t = -\partial F/\partial Q_{ji}$. Normally, Q is small in the isotropic phase, and hence the Q^3 and Q^4 terms and the $\chi_{ij}(\omega')E_i^*(\omega')E_j(\omega')$ term in Eq. (2) are often negligible. The dynamic equation assumes the form

$$\nu\frac{\partial Q_{ij}}{\partial t} + a(T - T^*)Q_{ij} = f_{ij}(t)$$

$$f_{ij} = \frac{1}{6}\Delta\chi(E_i^*E_j - \frac{1}{3}|E|^2\delta_{ij})(\omega,t) \qquad (3)$$

Consider first the steady-state solution of Eq. (3). If the optical field propagating along $\hat{z}$ is linearly polarized, e.g., $\vec{E} = E\hat{x}$, we find immediately

$$Q_{xx} = -2\,Q_{yy} = \frac{1}{9}\Delta\chi|E(\omega)|^2/a(T - T^*). \tag{4}$$

The corresponding induced linear birefringence at ω' is

$$\delta n_\ell(\omega') = (2\pi/n)\frac{2}{3}\Delta\chi(\omega')(Q_{xx} - Q_{yy})$$

$$= (2\pi/n)\,\Delta\chi(\omega)\,\Delta\chi(\omega')\,|E(\omega)|^2/9a(T - T^*) \tag{5}$$

where n is the linear refractive index. From the usual definition of the optical Kerr constant $B = \omega'\delta n_\ell/2\pi c|E(\omega)|^2$, we have

$$B = (\omega/nc)\,\Delta\chi(\omega)\,\Delta\chi(\omega')/9a(T - T^*). \tag{6}$$

If the intense optical field is elliptically polarized, e. g., $\vec{E}(\omega) = \hat{e}_+E_+ + \hat{e}_-E$ with $\hat{e}_\pm = (\hat{x} \pm i\hat{y})/\sqrt{2}$, we find from Eqs. (1) and (3) the following susceptibility tensor in the circular coordinates

$$\frac{1}{2}\begin{pmatrix} \chi_{xx} + \chi_{yy} + i(\chi_{xy} - \chi_{yx}), & (\chi_{xx} - \chi_{yy}) - i(\chi_{xy} + \chi_{yx}) \\ (\chi_{xx} - \chi_{yy}) + i(\chi_{xy} + \chi_{yx}), & \chi_{xx} + \chi_{yy} - i(\chi_{xy} - \chi_{yx}) \end{pmatrix}$$

$$= \bar{\chi}\delta_{ij} + \frac{(\Delta\chi)^2}{9a(T - T^*)}\begin{pmatrix} -\frac{1}{3}|E_+|^2 + \frac{2}{3}|E_-|^2 & E_-^*E_+ \\ E_-E_+^* & \frac{2}{3}|E_+|^2 - \frac{1}{3}|E_-|^2 \end{pmatrix}. \tag{7}$$

We can write

$$\chi_{ij}(\omega)E_i^*(\omega)E_j(\omega) = \bar{\chi}|E(\omega)|^2 + \delta\chi_+|E_+(\omega)|^2 + \delta\chi_-|E_-(\omega)|^2$$

$$\delta\chi_\pm = [(\Delta\chi)^2/9a(T - T^*)]\left(-\frac{1}{3}|E_\pm(\omega)|^2 + \frac{5}{3}|E_\pm(\omega)|^2\right) \tag{8}$$

and then the field-induced refractive indices seen by the two circular components of the incoming elliptically polarized light are

$$\delta n_\pm(\omega) = (2\pi/n)\delta\chi_\pm(\omega). \tag{9}$$

The corresponding circular birefringence is

$$\delta n_c = \delta n_- - \delta n_+$$

$$= (2\pi/n)2[(\Delta\chi)^2/9a(T - T^*)]\ [|\hat{e}_+^+\cdot\vec{E}(\omega)|^2 - |\hat{e}_-^+\cdot\vec{E}(\omega)|^2]. \tag{10}$$

We shall see later that the above-mentioned induced linear and circular birefringences can be deduced from measurements of phase shifts of linear and the elliptical polarizations respectively. As seen in the above expressions, all these field-induced refractive indices and birefringences diverge as T approaches T^*. This critically divergent behavior is of course characteristic of a pretransitional phenomenon. In liquid crystalline materials, the first-order transition temperature T_K ($>T^*$) always sets in before T reaches T^*.

In nonlinear optics, the field induced refractive indices can be described more generally from symmetry consideration.[4,5] For an isotropic medium, the third-order nonlinear polarization takes the form

$$P_i^{(3)}(\omega') = \sum_j 6\Big[\chi^{(3)}_{1122}(\omega' = \omega' + \omega - \omega)E_i(\omega')E_j(\omega)E_j^*(\omega) + \chi^{(3)}_{1212}(\omega' = \omega' + \omega - \omega)E_j(\omega')E_i(\omega)E_j^*(\omega) + \chi^{(3)}_{1221}(\omega' = \omega' + \omega - \omega)E_j(\omega')E_j(\omega)E_i^*(\omega)\Big] \tag{11}$$

where $\chi^{(3)}$'s are components of the third-order nonlinear susceptibility tensor. For $\omega = \omega'$, we have the circular coordinates

$$P_{\pm}^{(3)}(1) = 6\,(\chi^{(3)}_{1122} + \chi^{(3)}_{1212})|E_{\pm}(\omega)|^2 + (\chi^{(3)}_{1122} + \chi^{(3)}_{1212} + 2\chi^{(3)}_{1221})|E_{\mp}(\omega)|^2 E_{\pm}(\omega). \tag{12}$$

We then find for $\vec{E} = \hat{x}E$,

$$\delta n_{xx} = (2\pi/n)6(\chi^{(3)}_{1122} + \chi^{(3)}_{1212} + \chi^{(3)}_{1221})|E|^2$$
$$\delta n_{\ell} = (2\pi n)6(\chi^{(3)}_{1212} + \chi^{(3)}_{1221})|E|^2 \tag{13}$$

and for $\vec{E} = \hat{e}_+E_+ + \hat{e}_-E_-$

$$\delta n_{\pm} = (2\pi/n)6\left[(\chi^{(3)}_{1122} + \chi^{(3)}_{1212})|E_{\pm}(\omega)|^2 + (\chi^{(3)}_{1122} + \chi^{(3)}_{1212} + 2\chi^{(3)}_{1221})|E_{\mp}(\omega)|^2\right]$$

$$\delta n_c = (2\pi/n)12\chi^{(3)}_{1221}\left[|\hat{e}_+^{\dagger} \cdot \vec{E}(\omega)|^2 - |\hat{e}_-^{\dagger} \cdot \vec{E}(\omega)|^2\right]. \qquad (14)$$

Comparing Eqs. (13) and (14) with the previous expressions, we find, assuming $\Delta\chi(\omega) = \Delta\chi(\omega')$,

$$\chi^{(3)}_{1221} = -3\chi^{(3)}_{1122} = \frac{1}{6}\left[(\Delta\chi)^2/9a(T - T^*)\right]$$

$$\chi^{(3)}_{1212} = 0.$$

$$B = 6(\omega/nc)\chi^{(3)}_{1221} \qquad (15)$$

Owyong et al have shown that with only nuclear contribution, the third-order nonlinear polarization can be written as[6]

$$P_i^{(3)}(\omega) = \alpha E_i(\omega)E_j(\omega)E_j^*(\omega) + \beta E_j(\omega)E_j(\omega)E_i^*(\omega). \qquad (16)$$

In the case of liquid crystalline materials, this is true since the electronic contribution is negligible compared to the nuclear part. We then have

$$\alpha = 6\chi^{(3)}_{1122} = -\frac{1}{3}\beta$$

$$\beta = 6\chi^{(3)}_{1221}$$

$$B = (\omega/nc)\beta. \qquad (17)$$

We now consider the transient case where molecular ordering Q_{ij} is induced by an intense light pulse. From Eq. (3), we find immediately[1]

$$Q_{ij}(t) = \int_{-\infty}^{t} [f_{ij}(t')/\nu] e^{-(t - t')/\tau} \tag{18}$$

where the orientational relaxation time is defined as

$$\tau = \nu/a(T - T^*). \tag{19}$$

Consequently, we have

$$\delta n_{\ell}(t) = (2\pi c/\omega) B \frac{1}{\tau} \int_{-\infty}^{t} |E|^2(t') e^{-(t - t')/\tau} dt'$$

$$\delta n_{c}(t) = (2\pi c/\omega) 2B \frac{1}{\tau} \int_{-\infty}^{t} (|\hat{e}_{+} \cdot \vec{E}|^2 - |\hat{e}_{-} \cdot \vec{E}|^2)(t') e^{-(t - t')/\tau} dt'. \tag{20}$$

Thus, knowing the time variation of $\delta n_{\ell}(t)$ or $\delta n_{c}(t)$, we should be able to deduce the values of B and τ. Equation (19) shows that τ would diverge as T approaches T^*. This critical slowing-down behavior is again characteristic of a pretransitional phenomenon.

Suppose we have obtained B and τ as functions of temperature T. Then from Eqs. (15) and (19), we can deduce the parameters T^*, $(\Delta\chi)^2/a$, and ν/a. If, in addition, $\Delta\chi$ is separately measured, then a and hence ν are also known. Now, the Landau-deGennes model with the free-energy expression of Eq. (2) predicts[7] a first-order phase transition at

$T_K = T^* + 50b^2/243ad$ and an order parameter $Q_K = 20b/27d$ at the transition. Knowing T_K, T^*, a, and Q_K, we can then deduce b and d.

$$b = 18a(T_K - T^*)/5Q_K$$

$$d = 8a(T_K - T^*)T_K/Q_K^2. \qquad (21)$$

The validity of Eq. (21) however depends on whether the Landau model gives a valid description of the isotropic-nematic transition.

III. EXPERIMENTAL ARRANGEMENT AND DATA ANALYSIS

A. Sample Preparation.

Our experimental work was on seven homologous compounds of p,p'-di-n-alkoxy-azoxybenzenes. ($C_NH_{2N+1}O-C_6H_4-N_2O-C_6H_4-OC_NH_{2N+1}$ with N=1,2,---,7). The samples were purchased from Eastman Kodak Co. Purification of the samples was done by recrystalization from a saturated solution in various solvents (see Table II). The recrystallized sample was then placed in an optical cell 2.5 cm long and evacuated for several hours to remove atmospheric H_2O and O_2 and the residual solvent. After evacuation, the sample cell was sealed under vacuum. A sample prepared this way was very homogeneous and had a sharp isotropic-nematic transition. The transition temperature was constant to within 0.1°K for more than one month.

There was apparently a small amount of impurities in our samples as evidenced by the lower transition temperatures than those reported for pure samples in the literatures. The differences were typically less than 5°K,

suggesting an impurity concentration less than 1%. It appears that with such small impurity concentrations $(T_K - T^*)$ remains nearly unchanged. The temperature-dependent pretransitional properties as a function of $(T - T^*)$ should also remain unchanged and the material parameters deduced from our experiments should be insensitive to impurity contamination.[7]

During our optical measurements, the sample cell was placed in an oven with thermal control. The sample temperature was stablized to within 0.1°K and its uniformity throughout the cell was better than 0.2°K.

B. Experimental Techniques

We obtained the orientational relaxation time τ from the measurements of transient optical Kerr effect, and the nonlinear refractive index or optical Kerr constant from the measurements of intensity-dependent ellipse rotation. The details of the experimental arrangements have already been described elsewhere.[1] Here, for the sake of clarity, we have reproduced the schematics of the experimental arrangements for the two types of measurements in Fig. 1.

In the optical Kerr measurements, the main difference between the present setup and the earlier one is that here we used a weakly mode-locked ruby laser instead of a Q-switched laser. This was necessary because τ for the homologous compounds can be as small as few nsec. The mode-locked pulses had a pulsewidth of about 1 nsec. A single pulse of ~ 20 KW switched out from the mode-locked train was used in the measurements to induce molecular ordering, and a 10 mW CW He-Ne laser was used to

probe the ordering. In order to avoid any possible thermal lensing effect in the sample induced by the absorption of He-Ne laser light, a Pockell cell was employed to block the He-Ne laser beam until the arrival of the ruby laser pulse.

In the measurements of intensity-dependent ellipse rotation,[4] we used a single-mode Q-switched ruby laser. It had a pulsewidth of ~ 12 nsec and a peak power of ~ 100 KW. The beam was focused at the center of the sample cell. The length of the focal region was appreciably smaller than the cell length. With the output laser beam attenuated, the polarizer and the analyzer in Fig. 1b were set to be crossed to each other. The intensity-independent rotation of the elliptical polarization in the sample was then measured by the amount of light passing through the analyzer.

C. Data Analysis

In our optical Kerr measurements, the signal detected was the He-Ne laser light transmitted through the sample between crossed polarizers. The signal S^{OK} was therefore proportional to $\sin^2(\omega'\delta n_\ell \ell/2c)$ where ℓ is the sample length. The linear birefringence δn_ℓ was induced by a laser pulse according to Eq. (20). In our case, $\delta n_\ell \ell \ll 1$, and hence we have

$$S^{OK}(t) \propto \left[B \int_{-\infty}^{t} |E(t')|^2 e^{-(t - t')/\tau_{dt'}}\right]^2 \qquad (22)$$

where $|E(t)|^2$ is the exciting laser pulse. The above equation shows that if the laser pulsewidth is smaller than or comparable with τ, then at

sufficiently large t, the signal $S^{OK}(t)$ should decay exponentially as $\exp(-2t/\tau)$. This was indeed the case in our measurements. From the exponential tail, we could deduce the relaxation time τ. In principle, since the exciting pulse $|E(t)|^2$ is known from the oscilloscope trace, we should be able to deduce not only τ but also the optical Kerr constant B from the signal $S^{OK}(t)$. However, in the present case, the probing He-Ne laser beam was too weak to yield good signal-to-noise ratio for an accurate determination of B. We therefore used intensity dependent ellipse rotation measurements instead to determine B.

For an infinite plane wave, the intensity-dependent ellipse rotation θ across the cell is given by [1,4,6]

$$\theta = (\omega/2c)\delta n_c \ell. \tag{23}$$

For a focused beam, however, θ is a function of radius r. Assume a single-mode laser pulse with a Gaussian profile focused at z = 0.

$$|E|^2(r,z,t) = |\mathcal{E}_o|^2 \frac{W_o}{W^2(z)} \exp\left[-\frac{2r^2}{W^2(z)} - \alpha\left(z + \frac{\ell}{2}\right) - \gamma^2 t^2\right] \tag{24}$$

where $W^2(z) = W_o^2[1 + (2cz/\omega n W_o^2)^2]$, W_o is the minimum radius of the focus, α is the power attenuation coefficient due to scattering and linear loss, and γ is a constant. The sample cell extends from $z = -\ell/2$ to $z = \ell/2$. Following the analysis of Owyoung[6] using the paraxial approximation, we can describe each cylindrically symmetric set of rays in the focused beam by a parameter K

defined by

$$r^2 = KW^2(z). \tag{25}$$

For each set of rays, the ellipse rotation is

$$\theta_K(t) = \int_{-\ell/2}^{\ell/2} (\omega/2c)\delta n_c(K,z,t)$$
$$= (|\mathcal{E}_o|^2 \text{Cos } 2\phi)\, \frac{\pi^2 \omega n W_o^2}{c} BLg(t)e^{-2K} \tag{26}$$

where

$$L = \frac{2c}{\pi\omega n} e^{-\alpha\ell/2} \int_{-\ell/2}^{\ell/2} [e^{-\alpha z}/W^2(z)]dz$$

$$|\hat{e} \cdot \vec{E}|^2 - |\hat{e}_- \cdot \vec{E}|^2 = |E|^2 \text{ Cos } 2\phi$$

$$g(t) = \frac{\sqrt{\pi}}{2\gamma\tau} e^{-1/4\gamma^2\tau^2} [1 + \text{erf}(\gamma t - \frac{1}{2\gamma\tau})]e^{-t/\tau}. \tag{27}$$

If the attenuation length $(1/\alpha)$ is much smaller than the longitudinal focal dimension, $\omega n W_o^2/c$, then L can be approximated by

$$L = \frac{2}{\pi} e^{-\alpha\ell/2} [\tan^{-1}(c\ell/2\omega n W_o^2)] \tag{28}$$

which reduces to exp $(-\alpha\ell/2)$ when $\ell \gg \omega n W_o^2/c$ and to 1 if in addition $\ell \ll 1/\alpha$. We now have to integrate over all the rays in the beam to find the total power of the elliptically polarized light transmitted through the analzyer. In our case,

$\theta_K << 1$, and hence the measured signal is

$$S^{ER}(t) = \int_0^\infty (\sin 2\phi)^2 \theta_K^2(t) P_K(t) dK \tag{29}$$

where

$$P_K(t)dK = (nc/4\pi)|E|^2(r, z = \ell/2, t)2\pi r dr$$

$$= (ncW_o^2/4)|\mathcal{E}_o|^2 \exp(-2K - \alpha\ell - \gamma^2 t^2) dK.$$

We then have

$$S^{ER}(t) = \frac{\pi^4 n^3 \omega^2 W_o^6}{24c} |\mathcal{E}_o|^6 \sin^2 4\phi B^2 L^2 g^2(t) e^{-\alpha\ell - \gamma^2 t^2}. \tag{30}$$

Knowing $|\mathcal{E}_o|^2$ and ϕ, we can then determine the absolute value of the optical Kerr constant B.

In our experiment, we measured S^{ER}_{max} for the sample and used CS_2 as a reference whose Kerr constant is known. From Eq. (30), we find

$$B/B_{cs_2} = \left[\frac{S^{ER}_{max} e^{\alpha\ell} / L^2 \Gamma_{max} P_o^3}{(S^{ER}_{max} e^{\alpha\ell} / L^2 \Gamma_{max} P_o^3)_{cs_2}} \right]^{\frac{1}{2}} \tag{31}$$

where $\Gamma_{max} = [g^2(t) \exp(-\gamma^2 t^2)]_{max}$ and P_o is the incoming peak power. As seen from Eq. (30), S^{ER}_{max} is proportional to P_o^3. However, because of scattering and imperfect alignment, S^{ER}_{max} also has a residual term linear in P_o. Therefore, we must measure S^{ER}_{max} as a function of P_o and extract the term proportional to P_o^3 from the measurements.

We have measured τ, α, and B as functions of temperature in the isotropic phase for the seven homologous compounds of p,p'-di-n-alkoxy-azoxybenzenes. We have also found n and $\Delta\chi(= \delta\chi_{11}/Q_{xx})$ for these compounds using the wedge method of index refraction measurements[8] and the order parameters from magnetic resonance measurements.[9] Then, from Eqs. (6) and (19), we deduce the parameters ν, T^*, and a for each compound.

IV. EXPERIMENTAL RESULTS

In Figs. 2 and 3, we show, as examples, the results of our measurements of τ and B respectively as functions of temperature for two p,p'-di-n-alkoxy-azoxzybenzene compounds. Similar results were obtained for the other five compounds in the homologous series. In all cases, the data can be described very well by Eqs. (6) and (19). Strictly speaking, the viscoscity coefficient ν in Eq. (6) is not temperature-independent. One often expresses $\nu(T)$ in the form

$$\nu(T) = \nu_o \exp(-W/T) \qquad (32)$$

where W is a constant. However, in our cases, because the investigation was limited to a narrow temperature range, we can approximate $\nu(T)$ by $\nu(T_K)$. The error introduced by this approximation is less than 4%. Thus, by fitting the experimental data with the theoretical curves of Eqs. (6) and (19), we can deduce T^*, ν/a and $(\Delta\chi)^2/a$ for each compound. From the independently measured values of $\Delta\chi$,[8] we then obtain ν and a separately.

As discussed in Sec. II, if we believe in the Landau's expansion at the isotropic-nematic transition, we can also deduce the parameters b and d for these compounds using Eq. (21). Here, T_K's were measured, and the Q_K's were obtained from the linear birefringence measurements[8] normalized against the NMR results of Pines et al.[9] We have listed in Table III the values of $(T - T^*)\tau$, $(T - T^*)B$ and other parameters deduced from our measurements for the seven compounds of the homologous series. We have then plotted, as functions of the number of carbon atoms in the alkyl chain at either end of the molecule, $(T - T^*)\tau$ and $(T - T^*)B$ in Fig. 4, T^*, T_K, and ΔH in Fig. 5, ν and $\Delta\chi$ in Fig. 6, and a, b, and d in Fig. 7

In our relaxation measurements, shot noise in the photonmultiplier was the main source of experimental uncertainty. Typical error of about ± 10% is represented by the error bars in Fig. 2 where each data point was the result of average over more than 4 laser shots. This uncertainty can of course be improved by using a probe beam of stronger intensity. As the relaxation time τ approaches the response time of the detection system ($\lesssim$ 7 nsec in our case), the uncertainty would of course become larger unless the signal is properly deconvoluted.

The ellipse-rotation measurements had an accuracy better than 2% so far as the signal S_{max}^{ER}/P_o^3 was concerned. However, in deducing the optical Kerr constant from Eq. (31), the uncertainty in the relaxation time τ came in through g(t). Together with the uncertainty ($\sim$ ± 5%) in determing L, this led to an overall uncertainty of $\sim$ ± 15% in the values of B shown in Fig. 3.

V. DISCUSSION.

Figures 4 - 7 show how the increase of alkyl chain length by the addition of mythlene groups modifies the physical behavior of the homologous compounds. Here, we give a brief qualitative discussion of the results.

Figure 4 shows that the seven homologous compounds all have a large Kerr constant and a long relaxation time, which are characteristics of other liquid crystalline materials.[1] For the same $\Delta T = T - T^*$, $B\Delta T$ drops appreciably as N increases mainly due to a drop in $\Delta\chi$ shown in Fig. 6. On the other hand, $\tau\Delta T$ has a zig-zag behavior with increase of N. It is the result of the zig-zag behavior of ν also shown in Fig. 6.

In Fig. 5, we notice that a regular alteration of the isotropic-nematic transition temperatures T_K and T^* and the latent heat ΔH occurs between homologues containing odd and even numbers of carbon atoms in the alkyl chain. For T_K and ΔH, this is a common behavior for many homologous series of liquid crystalline compounds and is known to be the result of the cog-wheel arrangement of the carbon atoms along the alkyl chain. That the fictitious second-order transition temperature T^* also has such a behavior is a manifestation of the weak first-order transition characteristics of these compounds. Because of that, T_K and T^* never differ by more than 5°K. We also notice in Fig. 5 that $T_K - T^*$ becomes appreciably smaller for n = 6 and 7. This seems to suggest that the longer chains on the molecules make the transition closer to second order presumably due to the stronger waggling motion of the end segment and the falling off of the terminal interaction.

The vicosity coefficient ν shown in Fig. 6 also alters regularly between homologues containing odd and even numbers of carbon atoms in the alkyl chain. This is caused by the strong temperature dependence of ν as suggested in Eq. (32). In the present case, we can approximate $\nu(T)$ by $\nu(T_K)$. Then, according to Eq. (32), we expect to find smaller ν for compounds with large T_K and hence the qualitative behavior of ν in Fig. 6. However, we should not expect the constants ν_o and W in Eq. (32) to be the same for all the compounds in the homologous series. If they were, we would find log $\nu(T_K)$ versus T_K^{-1} to be a straight line from which we could deduce ν_o and W. As shown in Fig. 8, this is certainly not the case for the PAA homolgues.

The optical anistropy $\Delta\chi$ in Fig. 6 shows a fairly smooth decrease with increase of the chain length. In fact, on the microscopic scale, the molecular polarizability anisotropy $\Delta\alpha$ actually increases with the increase of chain length as one would expect intuitively.[8] The fact that $\Delta\chi$ behaves differently from $\Delta\alpha$ is because of the molar volume effect. The medium with longer chain molecules has a lower molecular density. Its effect on $\Delta\chi$ turns out to be larger than the incremental effect of $\Delta\alpha$ on $\Delta\chi$ due to addition of methylene group on the chain.

Figure 7 shows that the variations of the Landau parameters a, b, and d with chain length do not have any regular pattern. The physical meanings of a, b, and d often depend on the model describing the intermolecular interaction. In the mean-field theory of Maier and Saupe,[10] we should expect a to be a constant independent of the compounds. The values of a

for the seven homologous compounds in Fig. 7 however vary over a factor of 2. This suggests that the mean field theory for isotropic-nematic transition is actually a poor approximation. The values of b and d in Fig. 7 were deduced by assuming the Landau expansion of free energy is valid at the isotropic-nematic transition. To check the validity of the Landau expansion, we insert the values of a, b, and d in Eq. (2) with $Q \sim 0.4$ and $T = T_K$. We find that the b and d terms in Eq. (2) are often larger than the a term indicating a divergence or poor convergence of the power series expansion. Thus, at least the truncated Landau expansion in the form of Eq. (2) is not valid at $T = T_K$. The values of b and d given in Fig. 7 are therefore not very meaningful. For $T > T_K$ and $Q < 0.01$, however, Eq. (2) is valid. With the values of b and d given in Fig. 7, and for $Q < 0.01$, the b and d terms in Eq. (2) become negligible. This was true in our experiment where Q was always less than 10^{-3}.

In the literature, the Landau expansion has also been used to derive the heat content ΔH of a first-order transition

$$\Delta H = \frac{3}{4} a T_K Q_K^2 + \frac{5}{12} \left(\frac{\partial b}{\partial T}\right)_{T_K} Q_K^3 + \frac{9}{32} \left(\frac{\partial d}{\partial T}\right)_{T_K} Q_K^4. \qquad (33)$$

If we neglect the $\partial b/\partial T$ and $\partial d/\partial T$ terms, then we have

$$\Delta H = \frac{3}{4} a\ T_K Q_K^2. \qquad (34)$$

The above equation was used by Stinson et al.[7] Using the values of a, T_K, and Q_K listed in Tables I and III for the homologous compounds, we find the values of ΔH shown in Fig. 5 as ΔH_{th}. Compared with the directly measured values ΔH_{exp}, the agreement is fairly good for all compounds except N = 6 and 7. The discrepancy could be due to neglect of b and d terms in Eq. (33) or due to failure of the Landau expansion. It may also be the result of residual short-range smectic order at T_K since the N = 6 and N = 7 homologues are known to have a smectic phase at lower temperatures. The rapid rise of ΔH_{th} towards N = 6 and 7 comes from the corresponding sharp rise of a which in turn is the result of quick drop of $B(T - T^*)$ towards N = 6 and 7.

VI. CONCLUSION.

Using ellipse rotation and transient optical Kerr effect, we have measured the third-order nonlinear susceptibility (or the optical Kerr constant B) and the corresponding relaxation time τ for seven nematic compounds of the p, p'-di-n-alkoxy-azoxybenzene homologous series as functions of temperature in the isotropic phase. The results showing critical divergence of B and critical slowing down of τ are in good agreement with predictions from the Landau-deGennes' model. Similar in characteristics to other liquid crystalline materials, all these compounds have a large Kerr constant and a long relaxation time strongly dependent on temperature. Together with the existing data on optical anisotropy and the order parameter at the nematic-isotropic transition, we have deduced various characteristic parameters of the nematic compounds.

These include the fictitious second-order transition temperature T^*, the orientational viscosity ν, the Landau expansion coefficients a, b, and d, the heat content ΔH, etc. The results show how these characteristic parameters vary among the homologous series as the alkyl chain length of the molecules increases through addition of methylene groups to the chain. Part of the results can be understood from the molecular structural point of view. The variation of the Landau parameter a with compounds indicates that the mean field theory of Maier-Saupe is not a good approximation to describe the isotropic-nematic transition. Our values of a, b and d also suggest that the Landau series expansion of the free energy is a poor approximation at the transition. The heat contents ΔH derived from the expression $\Delta H = 3aT_K Q_K^2/4$ deviates appreciably from the experimental values for the higher members of the homologous series.

ACKNOWLEDGEMENT.

We want to thank Professor A. Pines and Dr. D. J. Ruben for letting us use their NMR results on order parameters prior to publication. We are grateful to the Material and Molecular Research Division of the Lawrence Berkeley Laboratory for providing us some of the experimental facilities. One of us (YRS) want to acknowledge the support of a research professorship at The Miller Institute of the University of California. Work performed under the auspices of the U. S. Energy Research and Development Administration.

REFERENCES

1. G. K. L. Wong and Y. R. Shen, Phys. Rev. Lett. 30, 895 (1973); Phys. Rev. A10, 1277 (1974); J. Prost and J. R. Lalanne, Phys. Rev. A8, 2090 (1973).

2. H. Arnold, Z. Phys. Chem. Leipzig 226, 146 (1964).

3. P. G. de Gennes, Phys. Lett. A30, 454 (1969) and Mol. Cryst. Liq. Cryst. 12, 193 (1971).

4. P. D. Maker and R. W. Terhune, Phys. Rev. 137, A801 (1965).

5. P. N. Butcher, "Nonlinear Optical Phenomena", (University Engineering Publications, Columbus, Ohio, 1965).

6. A. Owyoung, R. W. Hellworth, and N. George, Phys. Rev. B4, 2342 (1971); 5, 628 (1972); A Owyoung, IEEE J. Quantum Electron. QE-9, 1064 (1974).

7. T. W. Stinson and J. D. Litster, Phys. Rev. Lett. 25, 503 (1970); T. W. Stinson, J. D. Litster, and N. A. Clarke, J. Phys. (Paris) 33, 69 (1972).

8. E. G. Hanson and Y. R. Shen (to be published).

9. A. Pines, D. J. Ruben, and S. Allison, Phys. Rev. Lett. 33, 1002 (1974); More refined data are given by A. J. Pines and D. J. Ruben (to be published).

10. W. Maier and A. Saupe, Z. Naturf. A13, 564(1958); A14, 882 (1959); A15, 287 (1960).

FIGURE CAPTIONS

Fig. 1(a) Experimental arrangement for observing molecular orientational relaxation times in nematic liquid crystals. BS, beam splitter; P-1, P-2, P-3 linear polarizers; D-1, ITT F4018 fast photodiode; D-2, RCA photomultiplier 7102; F-1, neutral-density stacks.

(b) Experimental arrangement for observing ellipse-rotation effect. P-1, P-2, Glan polarizers; R-1, R-2, fresnel rhombs; L-1, L-2, 15-cm lenses; F-1, F-2, neutral-density stacks; D-1, D-2, ITT fast photodiodes.

Fig. 2 Experimental results on optical Kerr constants versus temperature for $C_NH_{2N} + 1O\text{-}C_6H_4\text{-}N_2O\text{-}C_6H_4\text{-}OC_nH_{2n} + 1$ with N = 1 and 7. The solid curves are calculated from Eq. (6).

Fig. 3 Experimental results on orientational relaxation times versus temperature for $C_NH_{2N} + 1O\text{-}C_6H_4\text{-}N_2O\text{-}C_6H_4\text{-}OC_NH_{2N} + 1$ with N = 1 and 7. The solid curves are calculated from Eq. (19).

Fig. 4 Experimental values of $(T - T^*)B$ and $(T - T^*)\tau$ for the first seven p, p'-di-n-alkoxy-azoxybenzene homologues.

Fig. 5 Experimental values of T_K, T^*, and ΔH_{exp} for the first seven p,p'-di-n-alkoxy-azoxybenzene homologues. The values of ΔH_{th} were deduced from Eq. (34) using experimental values of a, T_K, and Q_K.

Fig. 6 Values of ν and $\Delta\chi$ for the first seven p,p'-di-n-alkoxy-azoxybenzene homologues.

Fig. 7 Values of the Landau expansion coefficients a, b,and d (see Eq. (2)) deduced from the experiment for the first seven p,p'-di-n-alkoxy-azoxybenzene homologues.

Fig. 8 Plot of log ν versus T_K^{-1} showing that the experimental data do not fall on a straight line.

TABLE CAPTIONS

Table I. Molecular structures and other characteristic parameters of the p,p'-di-n-alkoxy-azoxybenzene homologues.

Table II. Solvents used for recrystallization of the p,p'-di-n-alkoxy-azoxybenzene homologous compounds.

Table III. Various characteristic parameters of the p,p'-di-n-alkoxy-azoxybenzene homologues deduced from the experiment.

TABLE I

Structure: $CH_3-(CH_2)_{N-1}-O-(C_6H_4)-N_2O-(C_6H_4)-O-(CH_2)_{N-1}-(CH_3)$

N	1	2	3	4	5	6	7
T_K(°C)	132.7	163.1	119.95	129.9	118.6	123.9	119.3
S_K	.400	.571	.395	.475	.358	.437	.431
$\Delta\chi$	108.9	97.1	87.2	79.0	74.9	64.5	60.9
ΔH_{exp}(10^6 erg/cm^3)	25.4	52.5	22.8	31.4	19.9	26.2	23.5

TABLE II

N	1 2	3	4	5 6 7
Solvent	1-pentanol	n-hexane	1-pentanol	acetone

TABLE III

N	1	2	3	4	5	6	7
$(T_K - T^*)(^\circ K)$	3.0	3.8	2.75	4.9	4.4	0.9	0.7
$\tau\Delta T(10^{-9}\text{sec}^\circ K)$	90	80	180	155	240	150	140
$B\Delta T(10^{-5}\text{esu})$	10.5	9.2	9.0	8.9	6.4	3.9	2.2
$\nu(10^{-3}\text{poise})$	62.6	52.1	95.9	68.9	135.4	105.1	151.3
$a(10^5\text{ergs/cm}^3{}^\circ K)$	6.69	6.52	5.33	4.45	5.57	7.00	10.81
$b(10^7\text{ergs/cm}^3)$	21.0	19.4	15.0	17.9	24.1	4.4	6.0
$d(10^7\text{ergs/cm}^3)$	41.1	27.3	29.7	29.1	49.4	6.9	10.1
$\Delta H_{th}(10^6\text{ergs/cm}^3)$	33.9	56.9	24.6	30.3	20.9	39.8	59.0

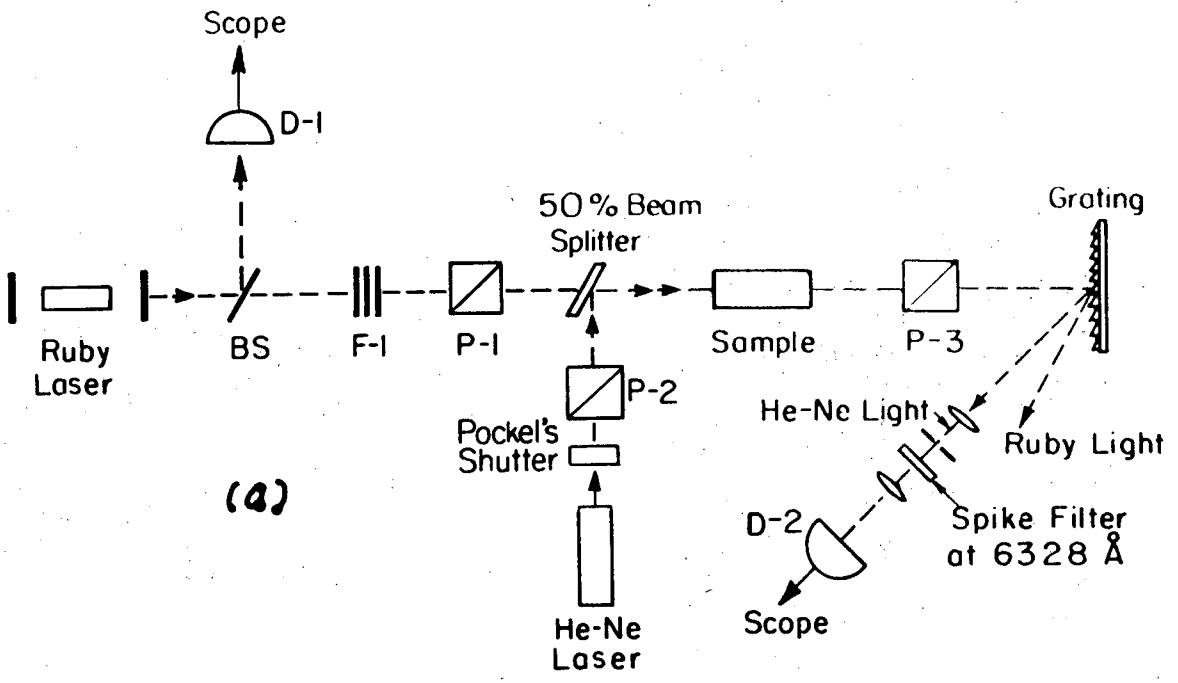
Scope
D-1
50% Beam Splitter
Grating
Ruby Laser
BS
F-1
P-1
Sample
P-3
P-2
Pockel's Shutter
He-Ne Light
Ruby Light
Spike Filter at 6328 Å
D-2
Scope
He-Ne Laser
XBL 743-5720

(a)

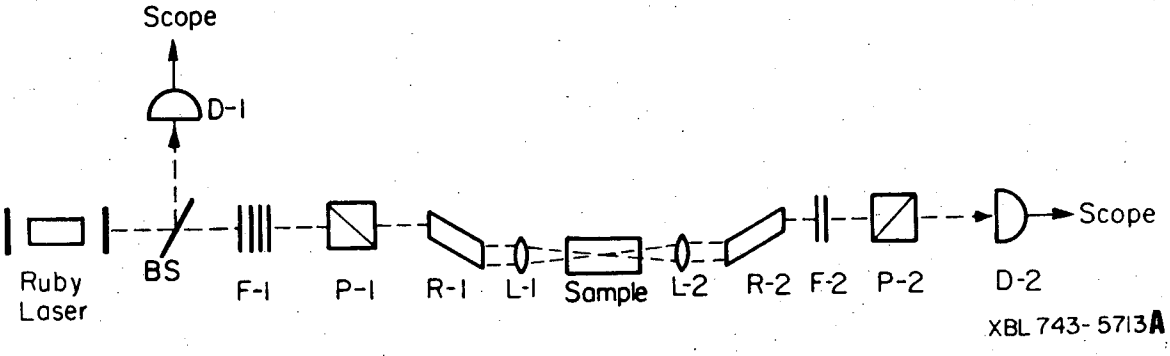
Scope
D-1
Ruby Laser
BS
F-1
P-1
R-1
L-1
Sample
L-2
R-2
F-2
P-2
D-2
Scope
XBL 743-5713A

(b)

Fig. 1

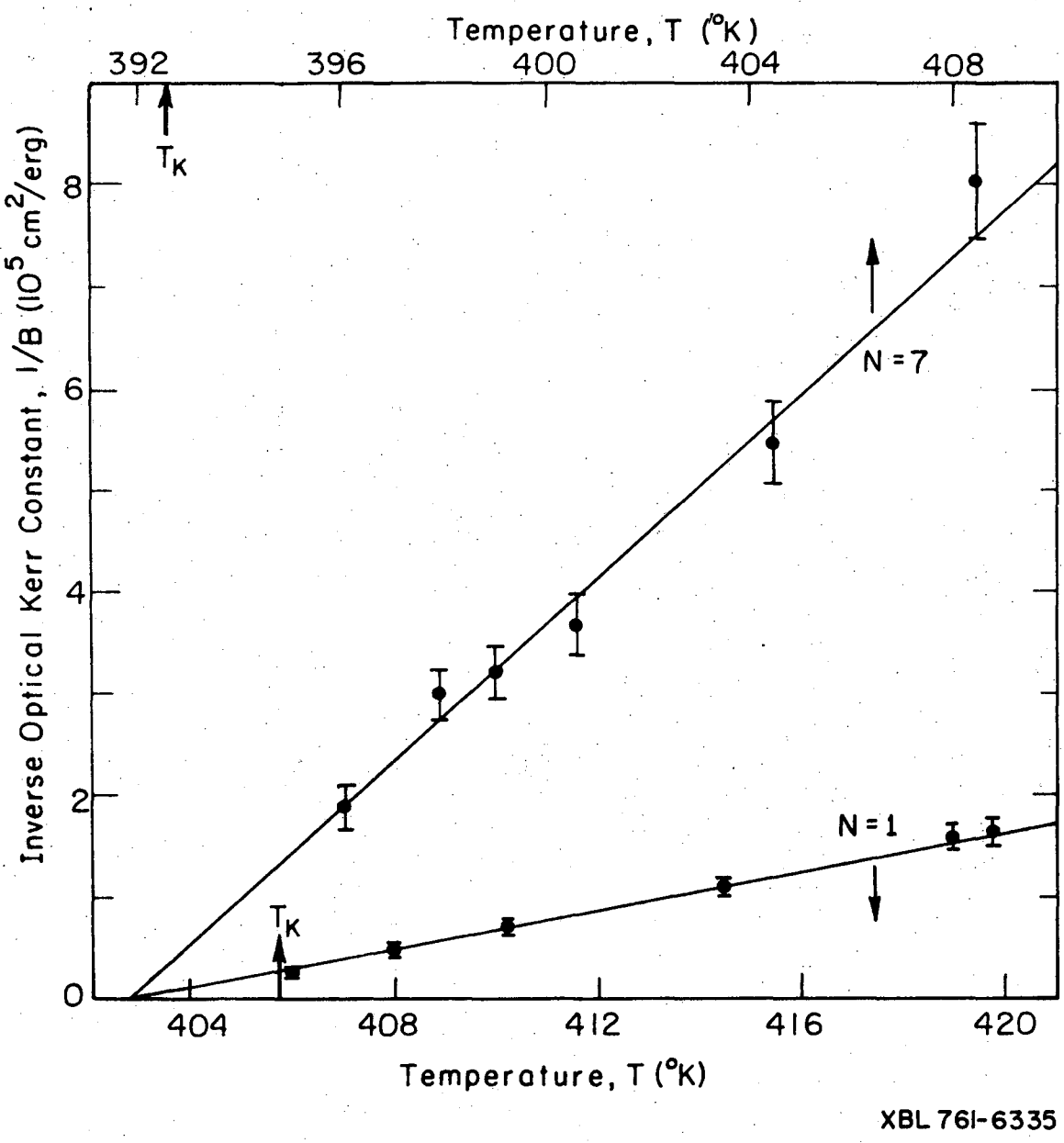
Temperature, T (°K)
392
396
400
404
408
T_K
Inverse Optical Kerr Constant, 1/B (10^5 cm^2/erg)
8
6
4
2
0
N = 7
N = 1
T_K
404
408
412
416
420
Temperature, T (°K)
XBL 761-6335

Fig. 2

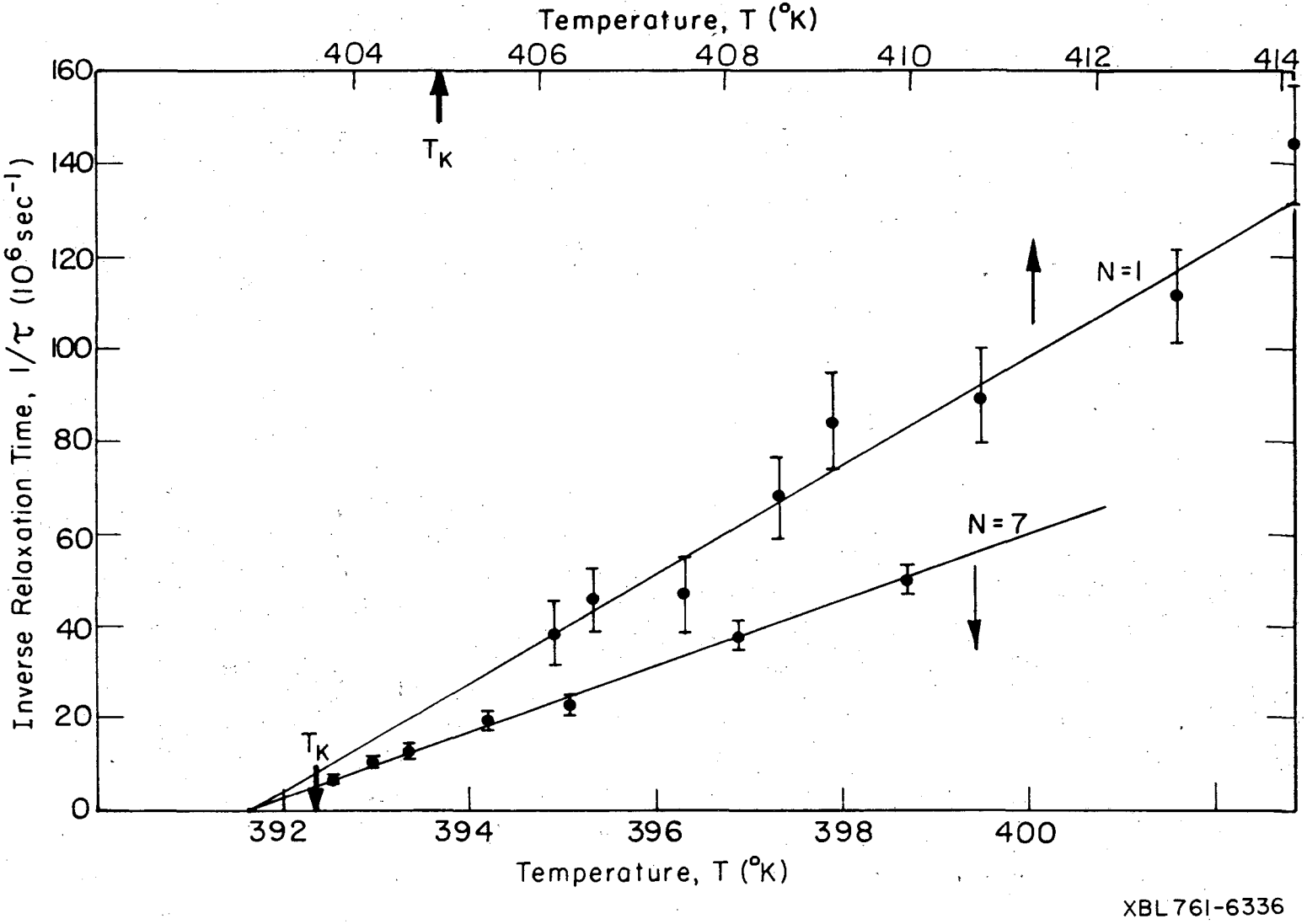

Fig. 3

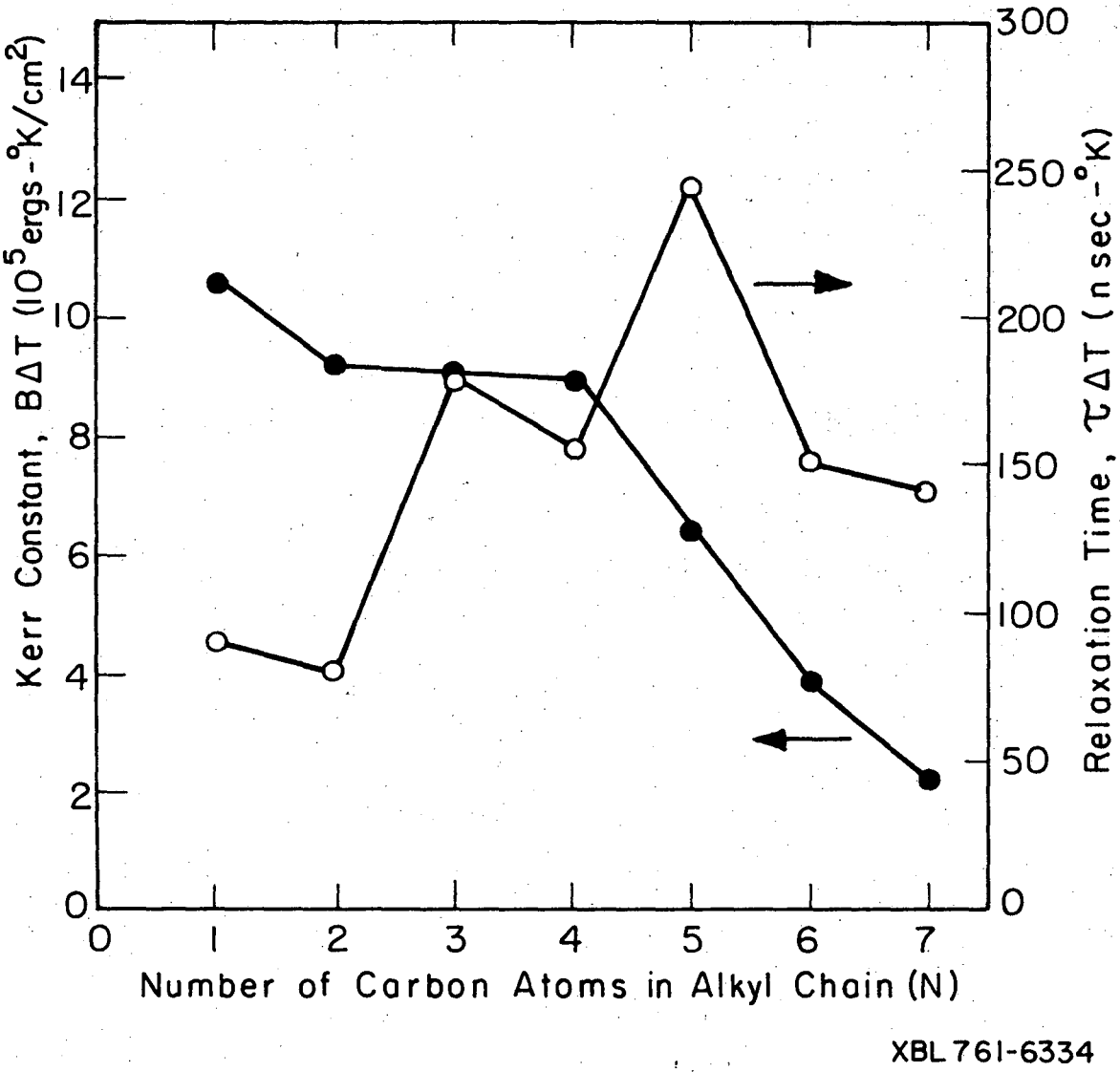
Kerr Constant, BΔT (10^5ergs-°K/cm^2)
Relaxation Time, τΔT (n sec-°K)
Number of Carbon Atoms in Alkyl Chain (N)
0
2
4
6
8
10
12
14
50
100
150
200
250
300
0
1
2
3
4
5
6
7
XBL 761-6334

Fig. 4

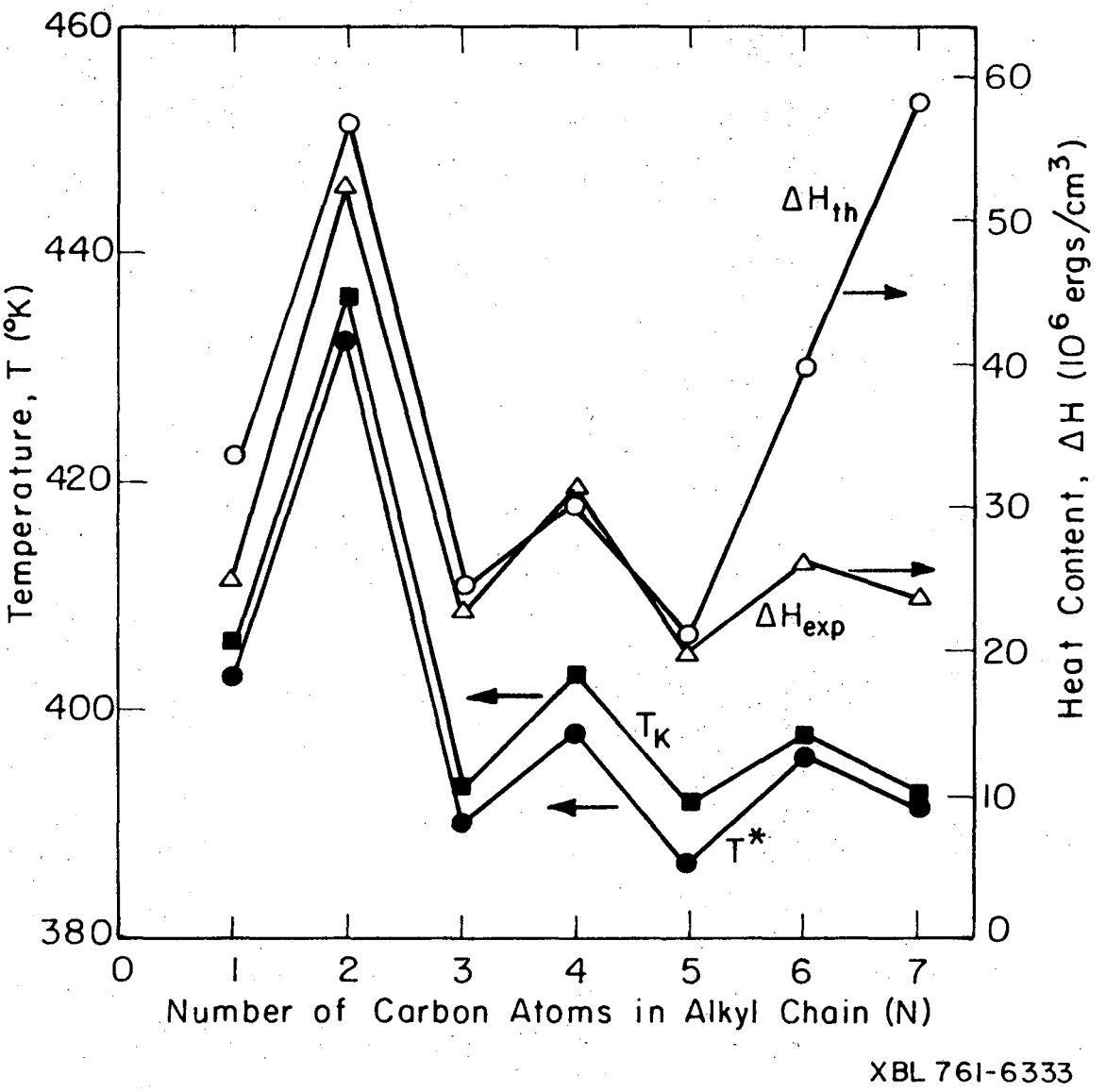

Fig. 5

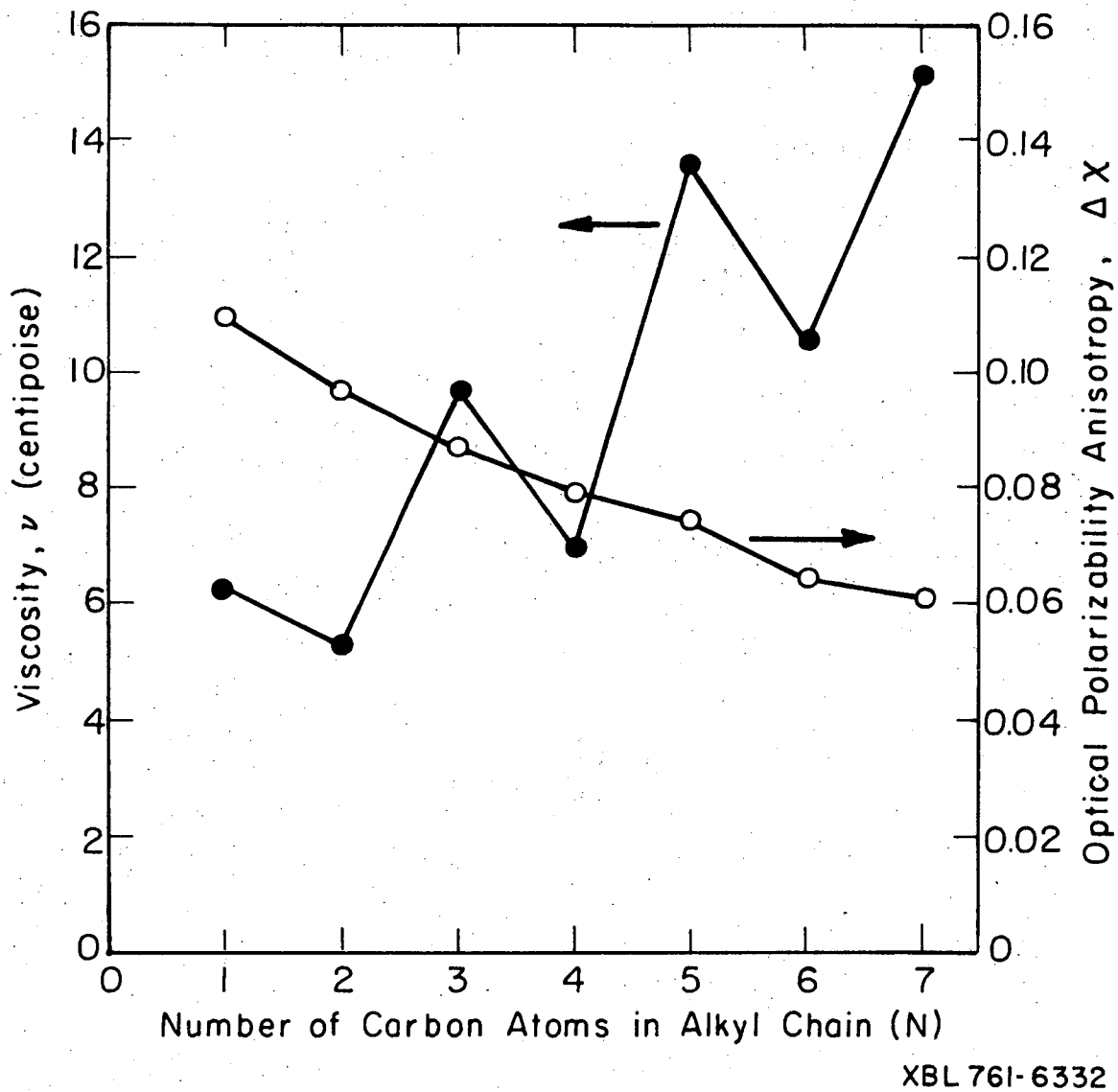
16
14
12
10
8
6
4
2
0
0.16
0.14
0.12
0.10
0.08
0.06
0.04
0.02
0
0 1 2 3 4 5 6 7
Viscosity, ν (centipoise)
Optical Polarizability Anisotropy, Δχ
Number of Carbon Atoms in Alkyl Chain (N)
XBL 761-6332

Fig. 6

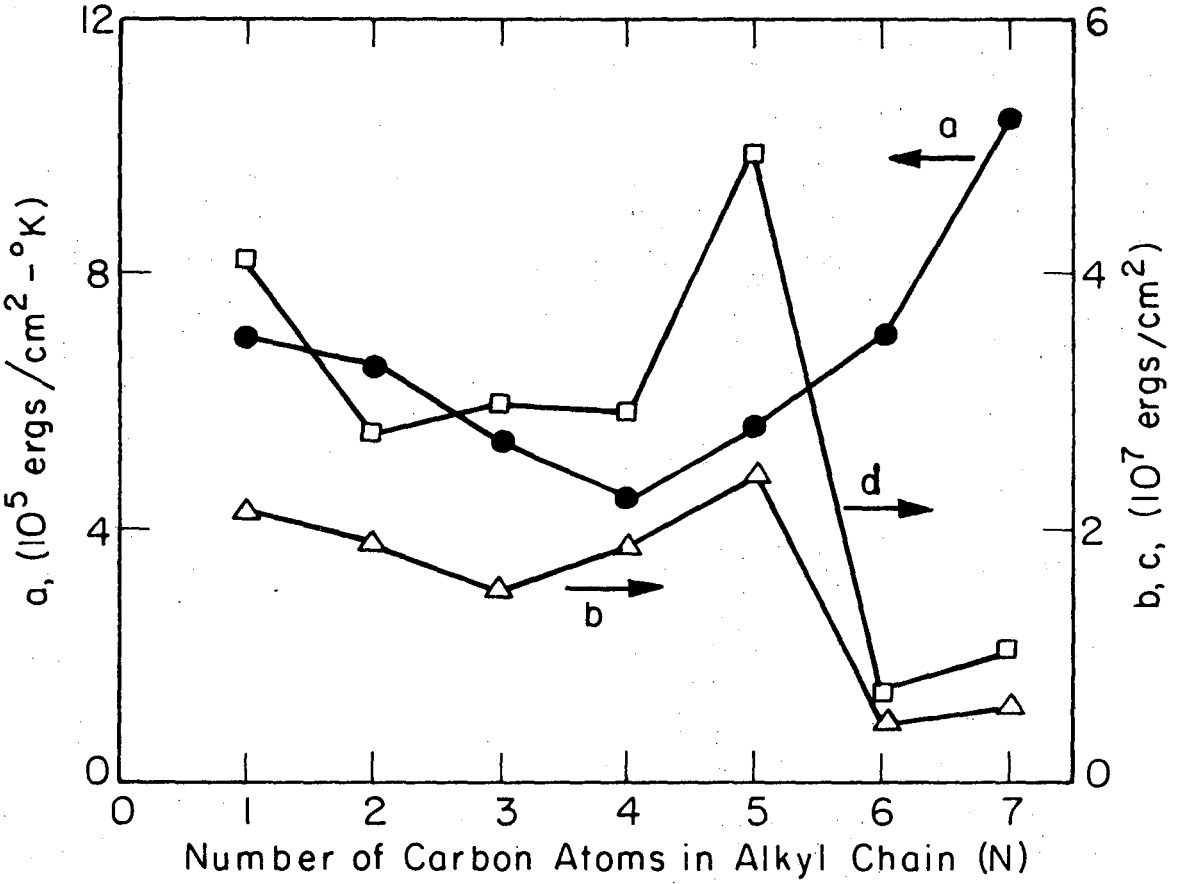

XBL 761-6330

Fig. 7

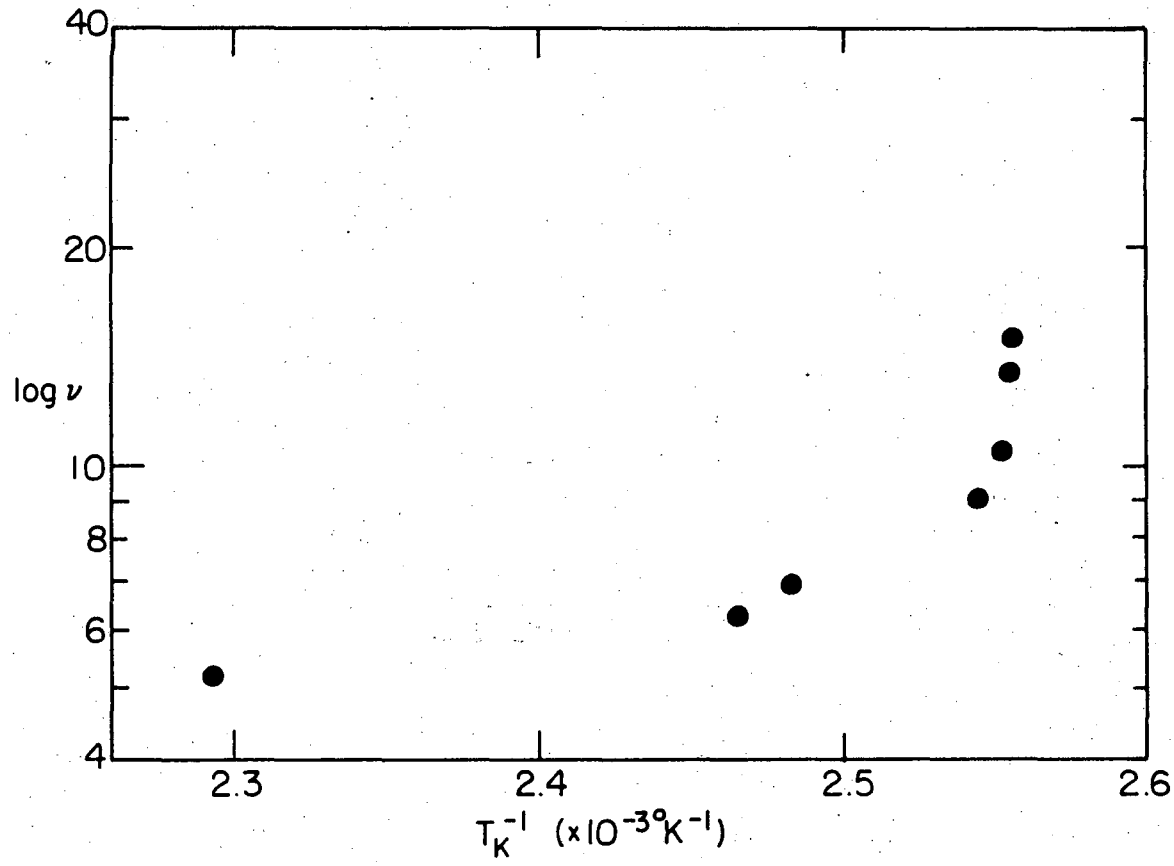

Fig. 8

TECHNICAL INFORMATION DIVISION
LAWRENCE BERKELEY LABORATORY
UNIVERSITY OF CALIFORNIA
BERKELEY, CALIFORNIA 94720